

# Stabilization of the inverted pendulum on a skate

D. Ambrosi and A. Bacciotti

Dipartimento di Matematica, Politecnico di Torino  
Corso Duca degli Abruzzi, 24 - 10129 Torino - Italy  
davide.ambrosi@polito.it, andrea.bacciotti@polito.it

## Abstract

In the classical control theory literature, the inverted pendulum stabilization problem has been addressed in two ways: as an application of the vibrational control principle, or by imagining that the pivot is on a cart moved according to a suitable feedback law. Several other stabilization methods have been recently proposed.

In this paper we propose a new approach: the pendulum is assembled on an ice skate, subject to some constraints and equipped with a driving device. The upper equilibrium position is stabilized provided that the speed of the skate is sufficiently large.

## 1 Introduction

The problem of stabilizing the upper equilibrium position of a pendulum (the so-called inverted pendulum problem) has attracted considerable attention in the control theory literature, both for its educational impact and the interest in applications: see for instance [2], [3], [8], [13], just to give an idea of the variety of possible approaches. Among them, we summarize the two most popular ones.

The first method is to exploit the so-called vibrational control principle [11], [14]. The basic idea is to displace the pivot of the pendulum along the vertical direction by applying an open-loop, oscillatory signal of high frequency and small amplitude.

The second approach applies to a pendulum in a plane: the pivot is moved in the horizontal direction (*the pendulum on the cart problem*, see for instance [15], [7]). In this case, a locally stabilizing control law in feedback form can be explicitly constructed.

In this paper we assume that the pivot of the pendulum is fixed to an ice skate moving in the horizontal plane. The skate is thought of as a segment, and it is equipped at its front endpoint with a control device which allows us to affect the direction of the motion. We show that such an inverted pendulum in the three-dimensional space can be stabilized by a suitably designed local feedback control law, provided that the speed of the skate is large enough.

Our approach to the inverted pendulum problem is manifestly inspired by the literature of the bicycle stability, for which we refer to the recent issue [1], and the review paper [12] (see especially the electronic supplementary material of [12], containing a historical review and an attempt of bibliographic classification). Indeed, in its crudest mechanical representation a bicycle is just an inverted pendulum and, in fact, even for a skilled rider it is very difficult to maintain the vertical position when the bicycle is at rest. On the contrary, when thrusting forward a bicycle at a sufficiently high speed, the vehicle can run for a long time while

maintaining the vertical position. This happens even though there is no rider and the bicycle is subject to large perturbations (see in [10] an indisputable experiment by Andy Ruina). This common experience shows that the stability of a bicycle is clearly related to its velocity and since the bicycle begun to diffuse as a popular mean of transport, many researchers have tried to give quantitative relations between stability and speed, giving rise to a very extensive literature.

Besides the gyroscopic effect, the basic motivations of a standard bicycle stability rest on a physical law and on a structural device: (a) the conservation of the angular momentum, and (b) the geometry of the front fork (in particular, the interplay between the rake and the leaning of the steer axis [6]). Roughly speaking, the sequence of events induced by the concurrent actions of (a) and (b) can be sketched as follows: when a bicycle leans right, the front wheel turns right too, the trajectory of the bicycle begins to bend on the same side, and the centrifugal force balances gravity thus restoring the vertical position.

In the present paper, the very simplified assembly we consider is formed by a pendulum and a skate, to be viewed as an ideal vehicle and modelled as a single rigid body. Of course, our “vehicle” has neither wheels nor steering front fork, so it is not able to keep the vertical position by itself, as the bicycle does. The control law we propose is actually designed in such a way to mimic the self-stability mechanism involving the centrifugal force and exploited by the standard bicycle.

The mathematical model for the pendulum and the skate, thought of as a single rigid body, is deduced in Section 2. It is simple enough to be accessible for qualitative analysis, but also as accurate as possible to match some relevant mechanical features of the system. The body is subject to two contact holonomic constraints and one non-slip nonholonomic constraint: in Section 3 we derive the equations of motion according to the d’Alembert principle. Their linearized versions around the equilibrium position are determined, as well. In Section 4, we introduce a control term in the equations, and the resulting system is analyzed from the point of view of control theory. As expected, the equilibrium position is unstable if the control term is set to be zero. Finally we propose our control law in the form of an output static feedback, characterized by a gain  $k$ . The stabilizability problem is addressed in Sections 5 and 6. In Section 5, we find the relation between  $k$  and the velocity of the vehicle, to be fulfilled in order to guarantee stability. Finally, in Section 6 we study the decay rate and show how it can be optimized by an appropriate choice of the gain  $k$ .

## 2 The mathematical model

### 2.1 Notation

In this work the assembly formed by the pendulum and the skate is modelled as a single rigid body with known mass and moments of inertia, constrained to move without friction on the horizontal plane (see Figure 1). The body is in contact with the ground at two points  $P$  and  $C$ , rear endpoint and front endpoint of the skate, respectively.

Moreover, we assume that the body can freely slip in  $C$ , while the point  $P$  can only move in the direction of the segment  $PC$ . The latter is a nonholonomic constraint, mimicking the blade of the skate and it is to be detailed below.

We denote by  $m$  the mass of the body and by  $B$  its center of mass. Let  $O$  be the point where the straight line issuing from  $B$  intersects orthogonally the straight line  $PC$ . Let finally  $b$  the length of the segment  $PO$  and  $h$  the length of the segment  $OB$ . We assume that  $O$  lies

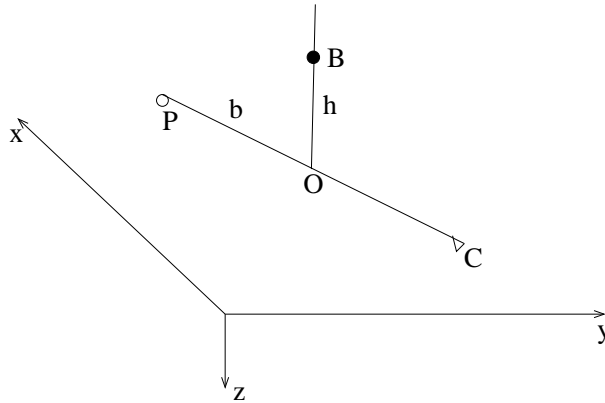


Figure 1: Main geometrical parameters of the body

between  $P$  and  $C$  and that  $P \neq O$  (while  $O = C$  is allowed). In particular we have  $b > 0$ . We assume also that  $h > 0$ . The point  $O$  can be thought of as the pivot of the pendulum, and  $h$  as its length.

The control device is located at  $C$ : it can apply in  $C$  a horizontal force directed orthogonally to the segment  $PC$ .

### 2.1.1 Positional and velocity variables

The rigid body introduced above is subject to two holonomic constraints and is therefore a system with four degrees of freedom. A convenient set of free coordinates can be introduced as follows.

Let  $(x, y, z)$  be a fixed reference frame and let  $(X, Y, Z)$  be a mobile one, centered in the point  $O$  and rotating so that axes are parallel to the principal axes of inertia of the body. The  $X$  axis is chosen to cross the two points  $P$  and  $C$  while the  $Z$  axis is directed toward the ground, so that a clockwise rotation is viewed as positive for a upstanding observer.

Convenient positional variables are (see Figure 2):

- the two horizontal coordinates of the point  $O$  in the  $(x, y)$  plane;
- the roll angle  $\theta$  measuring the rotation of the body around the  $X$  axis ( $\theta = 0$  corresponds to the vertical position of the body);
- the yaw angle  $\psi$  measuring rotations around  $z$  ( $\psi = 0$  corresponds to  $x = X$ ).

The point  $O$  moves in the  $xy$ -plane. We find convenient to represent its velocity as a pair  $(U, V)$  where the  $U$  component is measured along the  $X$ -axis, while the  $V$  component is orthogonal to the  $X$ -axis.

The components  $(\dot{x}, \dot{y})$  of the velocity of  $O$  and the quantities  $U$  and  $V$  are related by a pure rotation:

$$U = \dot{x} \cos \psi + \dot{y} \sin \psi , \quad V = -\dot{x} \sin \psi + \dot{y} \cos \psi . \quad (1)$$

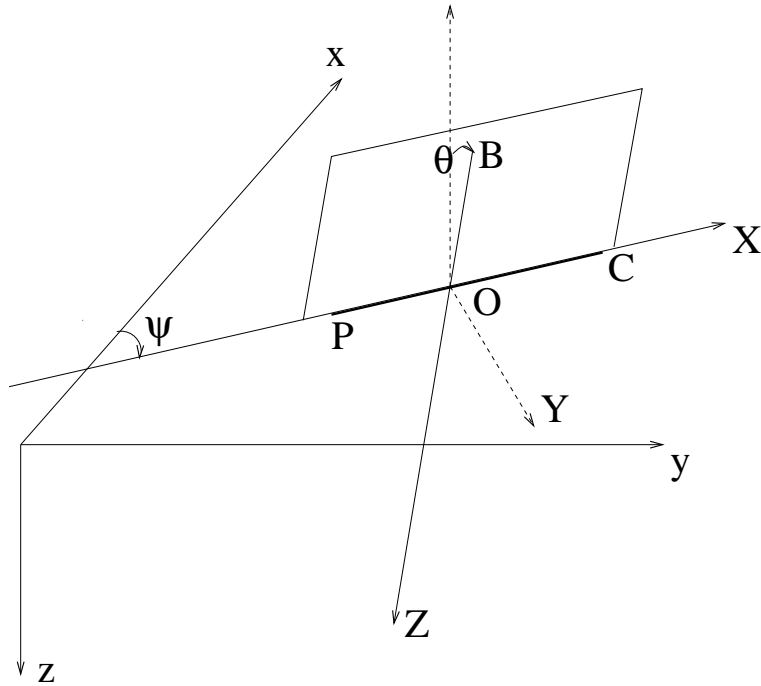


Figure 2: Fixed and rotating coordinate frames and plane of the main frame

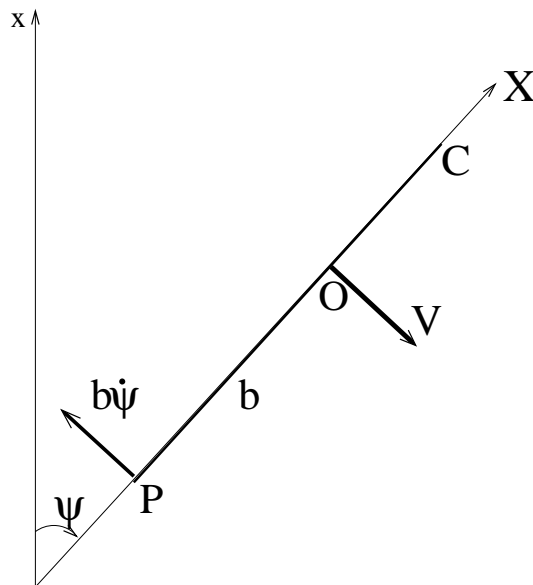


Figure 3: No-slip constraint on the rear endpoint : the velocity of the point  $P$  is the sum of the velocity of the point  $O$  plus the distance vector  $PO$  times the angular velocity  $\dot{\psi}$ : the constrain of null orthogonal displacement yields the relation (3).

For later use, we note that

$$\frac{\partial V}{\partial \psi} = -U, \quad \frac{\partial U}{\partial \psi} = V. \quad (2)$$

### 2.1.2 The nonholonomic constraint

The non-slip condition applied to the point  $P$  implies that the velocity vector of the point  $O$  is constrained to remain aligned with the segment  $PC$ . In other words, the velocity of  $O$  must have null component orthogonally to the  $X$  axis (see Figure 3). Recalling that the moving frame is centered at  $O$ , the corresponding kinematic relation at  $P$  reads:

$$\dot{x} \sin \psi - \dot{y} \cos \psi + b\dot{\psi} = -V + b\dot{\psi} = 0. \quad (3)$$

Relation (3) is a linear nonholonomic constraint in the velocity variables. It can be also written as

$$(\sin \psi, -\cos \psi, 0, b)(\dot{x}, \dot{y}, \dot{\theta}, \dot{\psi})^t = 0$$

where  $^t$  denotes transposition.

## 2.2 The Lagrangian functional

As friction is neglected in the present work, we can obtain the equations of motion in two ways: exploiting force and torque balance or combining in the Lagrange functional the expressions for the kinetic and potential energy. We adopt the latter approach, that keeps equations in a more compact form until derivatives are carried out. Interpretation of the resulting equations in terms of force balance will follow *a posteriori*. At this step, we neglect the control action, which will be included later in the model.

The velocity of the center of mass  $B$  of the vehicle is the sum of the velocity of the point  $O$  and the rotational contributions due to roll and yaw. Therefore we get:

$$\mathbf{v} = \left( U - h\dot{\psi} \sin \theta, V + h\dot{\theta} \cos \theta, h\dot{\theta} \sin \theta \right)^t. \quad (4)$$

The angular velocities  $\dot{\theta}, \dot{\psi}$  are not oriented according to the principal axis of inertia of the system and it is therefore convenient to decompose them into such directions to write suitably the contribution to the kinetic energy due to the rotation around the center of mass. Simple geometrical considerations lead to:

$$\begin{aligned} \omega_X &= \dot{\theta}, \\ \omega_Y &= \dot{\psi} \sin \theta, \\ \omega_Z &= \dot{\psi} \cos \theta. \end{aligned} \quad (5)$$

where  $(\omega_X, \omega_Y, \omega_Z)$  are the components of the angular velocity of the rigid body in the directions of the principal inertia axes, oriented like the mobile reference frame. The kinetic energy of the system can now be written as:

$$T = \frac{m}{2} |\mathbf{v}|^2 + \frac{1}{2} [I_X \omega_X^2 + I_Y \omega_Y^2 + I_Z \omega_Z^2], \quad (6)$$

where  $I_X, I_Y, I_Z$  are the principal inertia moments of the body with respect to  $B$ . Using the free coordinates  $\theta, \psi$  and the quantities  $U, V$ , we have

$$T = \frac{m}{2} \left( U^2 + V^2 + h^2 \dot{\theta}^2 + h^2 (\dot{\psi} \sin \theta)^2 + 2hV\dot{\theta} \cos \theta - 2hU\dot{\psi} \sin \theta \right) + \frac{1}{2} \left[ I_X \dot{\theta}^2 + I_Y (\dot{\psi} \sin \theta)^2 + I_Z (\dot{\psi} \cos \theta)^2 \right], \quad (7)$$

while the potential energy takes the simple form

$$E_p = mgh \cos \theta, \quad (8)$$

the force of gravity being for the moment the only external force acting on the system. The Lagrangian functional is, by definition,

$$\mathcal{L}(\theta, \psi, \dot{x}, \dot{y}, \dot{\theta}, \dot{\psi}) = T - E_p. \quad (9)$$

For notational and computational ease, it is convenient to view  $\mathcal{L}$  as the composition

$$\mathcal{L}(\theta, \psi, \dot{x}, \dot{y}, \dot{\theta}, \dot{\psi}) = F(\theta, \dot{\theta}, \dot{\psi}, U(\psi, \dot{x}, \dot{y}), V(\psi, \dot{x}, \dot{y}))$$

where  $F : \mathbf{R}^5 \rightarrow \mathbf{R}$  and  $U, V$  are given in (1).

### 3 The equations of motion

In this section we deduce the equations of the *nonholonomic dynamics* (*Lagrange-d'Alembert equations*) for our system, according to the d'Alembert principle of virtual displacements [5].

#### 3.1 The Lagrange-d'Alembert equation

The Lagrange-d'Alembert equations for the Lagrangian (9) under constraint (3) are

$$\frac{\partial \mathcal{L}}{\partial x} - \frac{d}{dt} \left( \frac{\partial \mathcal{L}}{\partial \dot{x}} \right) = -\frac{d}{dt} \left( \frac{\partial F}{\partial U} \frac{\partial U}{\partial \dot{x}} + \frac{\partial F}{\partial V} \frac{\partial V}{\partial \dot{x}} \right) = -\mu \sin \psi \quad (10)$$

$$\frac{\partial \mathcal{L}}{\partial y} - \frac{d}{dt} \left( \frac{\partial \mathcal{L}}{\partial \dot{y}} \right) = -\frac{d}{dt} \left( \frac{\partial F}{\partial U} \frac{\partial U}{\partial \dot{y}} + \frac{\partial F}{\partial V} \frac{\partial V}{\partial \dot{y}} \right) = \mu \cos \psi \quad (11)$$

$$\frac{\partial \mathcal{L}}{\partial \theta} - \frac{d}{dt} \left( \frac{\partial \mathcal{L}}{\partial \dot{\theta}} \right) = \frac{\partial F}{\partial \theta} - \frac{d}{dt} \left( \frac{\partial F}{\partial \dot{\theta}} \right) = 0 \quad (12)$$

$$\frac{\partial \mathcal{L}}{\partial \psi} - \frac{d}{dt} \left( \frac{\partial \mathcal{L}}{\partial \dot{\psi}} \right) = \frac{\partial F}{\partial U} \frac{\partial U}{\partial \psi} + \frac{\partial F}{\partial V} \frac{\partial V}{\partial \psi} - \frac{d}{dt} \left( \frac{\partial F}{\partial \dot{\psi}} \right) = -\mu b \quad (13)$$

where the multiplier  $\mu = \mu(t)$  is to be determined. Equations (10–13) together with (3), form the system to be solved. Equations (10) and (11) can be rewritten as

$$-\frac{d}{dt} \left( \frac{\partial F}{\partial U} \right) \cos \psi + \frac{\partial F}{\partial U} \dot{\psi} \sin \psi + \frac{d}{dt} \left( \frac{\partial F}{\partial V} \right) \sin \psi + \frac{\partial F}{\partial V} \dot{\psi} \cos \psi = -\mu \sin \psi \quad (14)$$

$$-\frac{d}{dt} \left( \frac{\partial F}{\partial U} \right) \sin \psi - \frac{\partial F}{\partial U} \dot{\psi} \cos \psi - \frac{d}{dt} \left( \frac{\partial F}{\partial V} \right) \cos \psi + \frac{\partial F}{\partial V} \dot{\psi} \sin \psi = \mu \cos \psi. \quad (15)$$

Adding (14) multiplied by  $-\sin \psi$  to (15) multiplied by  $\cos \psi$ , we get

$$\mu = -\frac{\partial F}{\partial U}\dot{\psi} - \frac{d}{dt} \left( \frac{\partial F}{\partial V} \right) . \quad (16)$$

On the other hand, adding (14) multiplied by  $\cos \psi$  to (15) multiplied by  $\sin \psi$ , we get

$$\frac{\partial F}{\partial V}\dot{\psi} - \frac{d}{dt} \left( \frac{\partial F}{\partial U} \right) = 0 . \quad (17)$$

Computing the partial derivatives explicitly and using the constraint (3), equation (12) rewrites as follows

$$\begin{aligned} (mh^2 + I_X)\ddot{\theta} - mgh \sin \theta \\ = -mhb\ddot{\psi} \cos \theta + mh^2\dot{\psi}^2 \sin \theta \cos \theta - mhU\dot{\psi} \cos \theta + I_Y\dot{\psi}^2 \sin \theta \cos \theta - I_Z\dot{\psi}^2 \sin \theta \cos \theta . \end{aligned} \quad (18)$$

Finally, we replace the Lagrange multiplier  $\mu$  in equation (13) by the relation (16). Using (2), (3) we have

$$\begin{aligned} \frac{d}{dt} \left( mh^2\dot{\psi} \sin^2 \theta - mhU \sin \theta + I_Y\dot{\psi} \sin^2 \theta + I_Z\dot{\psi} \cos^2 \theta + mb^2\dot{\psi} + mhb\dot{\theta} \cos \theta \right) \\ = -mbU\dot{\psi} - mhU\dot{\theta} \cos \theta . \end{aligned} \quad (19)$$

Equations (18) and (19) represent the angular momentum balance with respect to the  $X$  and  $Z$  axis, respectively.

### 3.1.1 Equilibrium position and linearization

Equations (18) and (19) read as a nonlinear system of ordinary differential equations. The first step in its investigation is the determination and characterization of possible equilibrium points.

Roughly speaking, if  $E$  is an equilibrium position of a given dynamical system, we say that  $E$  is *stable* if for each future time the trajectories remain in an arbitrarily small neighborhood of  $E$ , provided that the initial state lies in a sufficiently small neighborhood of  $E$ . If in addition the trajectories approach  $E$  asymptotically for  $t \rightarrow +\infty$ , then  $E$  is *asymptotically stable*. When the system is not stable, one says that it is *unstable* (more formal and detailed definitions can be found in many books: see for instance [4], [7] for expositions strictly related to control purposes).

The equilibrium positions of the system formed by (18), (19) can be found by setting  $\dot{\theta} = \dot{\psi} = \ddot{\theta} = \ddot{\psi} = 0$ , and solving the resulting equations in terms of the remaining variables. In particular,  $\theta = 0$  is an equilibrium position regardless the values of  $\psi$  and  $U$ . When  $\theta = 0$  the pendulum is in vertical position and this is just the equilibrium position whose stability is of interest in this paper.

Since our analysis is local, the theorem of stability at the first approximation applies (see for instance [7]). Linearizing around the equilibrium position

$$\theta = \dot{\theta} = \dot{\psi} = \ddot{\theta} = \ddot{\psi} = 0 , \quad (20)$$

(18) and (19) simplify to

$$J_0\ddot{\theta} - mgh\theta = -mhb\ddot{\psi} - mhU\dot{\psi} \quad (21)$$

$$\frac{d}{dt} \left( L\dot{\psi} - mhU\theta + mhb\dot{\theta} \right) = -mbU\dot{\psi} - mhU\dot{\theta} \quad (22)$$

where  $J_0 = I_X + mh^2$  and  $L = I_Z + mb^2$ . The explicit form of (17) is

$$\dot{U} = h\ddot{\psi} \sin \theta + 2h\dot{\theta}\dot{\psi} \cos \theta + b\dot{\psi}^2 . \quad (23)$$

Its linearized version simply states that  $U$  remains constant around the equilibrium position (20). In other words, since energy is conserved, small variations of  $\theta$  (i.e., of the height of point  $B$ ) are balanced by lateral displacements of  $O$ .

As far as we investigate the linearized equation (21–22),  $U$  is constant. Notice that the actual value of  $\psi$  at the equilibrium position is irrelevant. The value of  $U$ , which determines the cruising speed of the vehicle, is assumed to be positive: it is going to play the role of a crucial parameter in our forthcoming discussion.

Since  $U$  is constant, equation (22) can be integrated, which yields  $L\dot{\psi} = -mhb\dot{\theta} - mbU\psi + C$ , where  $C$  is a real constant. Without loss of generality, we can assume that initially  $\psi = 0$ . Hence, the unique choice compatible with the equilibrium position (20) is  $C = 0$ . Thus we have

$$L\dot{\psi} = -mhb\dot{\theta} - mbU\psi . \quad (24)$$

## 4 The control device

In the present paper the control enters as an external force which enables to govern the direction of the motion. Thus, it will be appended as an additional term  $w$  to the linearized equation (22) of the nonholonomic motion which (with  $U$  constant) becomes

$$L\ddot{\psi} + mhb\ddot{\theta} = -mbU\dot{\psi} + w . \quad (25)$$

The system formed by (21), (25) can be rewritten in normal form, provided that  $D = LJ_0 - m^2h^2b^2 \neq 0$ :

$$\begin{cases} \ddot{\theta} = \frac{1}{D} \left( mghL\theta - mhUI_Z\dot{\psi} - mhbw \right) \\ \ddot{\psi} = \frac{1}{D} \left( -m^2h^2gb\theta - mbUI_X\dot{\psi} + J_0w \right) \end{cases} \quad (26)$$

or, as a first order system,

$$\dot{\xi} = A\xi + Bw \quad (27)$$

where  $\xi = (\theta, \dot{\theta}, \psi, \dot{\psi}) \in \mathbf{R}^4$ . The matrices  $A, B$  (of dimension  $4 \times 4$  and  $4 \times 1$ , respectively) are easily computed from (26).

**Proposition 1** *System (26) with  $w = 0$  is unstable.*

**Proof**

The characteristic polynomial of matrix  $A$  is

$$\lambda^4 + \frac{mbUI_X}{D}\lambda^3 - \frac{mghL}{D}\lambda^2 - \frac{m^3h^3gbUI_Z + m^2gbhLUI_X}{D^2}\lambda.$$

There is a root  $\lambda = 0$ . Moreover, according to the Routh-Hurwitz criterion, at least one of the remaining roots has a positive real part. ■

The use of the control is therefore essential in order to achieve stability. We propose to define  $w$  in the following specific form:

$$w = \kappa_1(\dot{\psi}) + \kappa_2(\dot{\theta}) \quad (28)$$

where  $\kappa_1(\dot{\psi}) = mbU\dot{\psi}$  and  $\kappa_2(\dot{\theta}) = k\dot{\theta}$ , and  $k$  is a real parameter to be suitably chosen. The purpose of this control law is twofold.

- (1) By virtue of  $\kappa_1(\dot{\psi})$ , the term at the right-hand-side of (25) cancels. This will enable us to decouple (21), (25), reducing the problem to a simple second order equation in the unknown  $\theta$ .
- (2) By an appropriate choice of the gain  $k$ , the term  $\kappa_2(\dot{\theta})$  stabilizes the system and it is expected to improve the decay rate.

These ideas will be developed and made more precise in the Sections 5 and 6.

**Remark 1** *A control law which depends on some (but not all) the state variables of the system is a particular case of what is called, in the control theory literature, an output static feedback. In particular, the control law (28) can be classified as an output static feedback provided that  $(\dot{\theta}, \dot{\psi})$  are assumed as output variables.*

*In case of practical implementation, this choice of the output variables has the disadvantage of requiring sensors for velocity measurement. However, as already mentioned, it enables us to decouple the system and to pursue a satisfactory stability analysis, and this is a great theoretical advantage.*

## 5 Stability analysis

With the control law (28), equation (25) becomes

$$L\ddot{\psi} = -mhb\ddot{\theta} + k\dot{\theta}. \quad (29)$$

On the other hand, continuing to assume zero initial conditions, (29) can be integrated, thus giving

$$L\dot{\psi} = -mhb\dot{\theta} + k\theta. \quad (30)$$

Finally, replacing (29) and (30) in (21) yields

$$J\ddot{\theta} + \frac{mhb}{L}(k - mhU)\dot{\theta} + mh\left(\frac{Uk}{L} - g\right)\theta = 0 \quad (31)$$

where

$$J = mh^2 + I_X - \frac{m^2 h^2 b^2}{L} = J_0 - \frac{m^2 h^2 b^2}{L}. \quad (32)$$

Equation (31) is the basis for our stability analysis. Let

$$r(U) = mhU, \quad k_0(U) = \frac{Lg}{U}.$$

Note (see Figure 4) that the graphs of  $r(U)$  and  $k_0(U)$  intersect at

$$U = U_1 = \sqrt{\frac{gL}{mh}}. \quad (33)$$

**Theorem 1** *The equilibrium position  $\theta = \dot{\theta} = 0$  of the equation (31) is asymptotically stable for each  $k$  such that*

$$k > \max \{r(U), k_0(U)\} \quad (34)$$

**Proof** Let us first remark that

$$J = I_X + mh^2 \left( 1 - \frac{mb^2}{I_Z + mb^2} \right) > 0.$$

Then, the equilibrium position  $\theta = \dot{\theta} = 0$  is asymptotically stable if and only if the remaining two coefficients of (31) are both positive. This happens if and only if (34) holds. ■

**Remark 2** *For  $k = r(U)$ , the dissipative term in (31) vanishes. The equilibrium is unstable if  $U \leq U_1$  and stable (not asymptotically) in the opposite case. If  $k = k_0(U)$ , equation (31) has infinitely many equilibria. They are all stable (not asymptotically) if and only if  $U \leq U_1$ . Note that these conclusions involve eigenvalues with zero real part: in general they cannot be extended to the original nonlinear system.*

**Remark 3** *Relation (24) shows how the feedback law (28) works: it forces the yaw angle  $\psi$  to depend on the roll angle  $\theta$ . Note that because of (34), when  $U = 0$  the system cannot be stabilized by feedback laws of the form (28).*

## 6 Improving the decay rate

For asymptotically stable systems, it is important to evaluate the *decay rate*, which determines how rapidly a solution resulting from a perturbed initial state re-approaches the assigned equilibrium position. In fact, for many applications the purpose of feedback control is not only to provide asymptotic stability, but also to make the decay as fast as possible. For linear systems, the achievement of arbitrarily fast decay is equivalent to the so-called "pole placement" problem.

It is well known that arbitrary pole placement is possible provided the system is controllable and a full state static feedback is available, but this is in general not possible under output static feedback. As a matter of fact, the basic condition for arbitrary pole placement

under output static feedback<sup>1</sup> is not satisfied in our case [9]. Therefore, it becomes crucial to investigate the maximal decay rate achievable under output feedback of the form (28). To this aim, we need to compute explicitly the characteristic roots of (31), that is the solutions of the second order polynomial equation

$$\lambda^2 + \frac{mhb}{JL}(k - mhU)\lambda + \frac{mh}{J} \left( \frac{Uk}{L} - g \right) = 0. \quad (35)$$

**Definition 1** *The decay rate  $\mu$  is defined as the maximum real part among the roots of the second order polynomial equation (35). Hence, if the roots are real, say  $\lambda_1, \lambda_2$  with  $\lambda_1 \leq \lambda_2$ , we have  $\mu = \lambda_2$ ; if the roots are complex conjugate, then  $\mu$  coincides with the common real part of  $\lambda_1$  and  $\lambda_2$ .*

The decay rate  $\mu$  depends on all the parameters  $m, h, b, U, I_Z, I_X$  of the system and, in addition, on the gain  $k$ . In what follows, we are primarily interested in studying the dependence of  $\mu$  on  $k$ , i.e., we address the problem to design the applied feedback law in such a way to improve the stability performance in terms of decay rate. For this reason, from now on we will write  $\mu(k)$ . However, also the dependence of  $\mu$  on  $U$  will be taken into account. Let us denote

$$U_0 = \sqrt{\frac{mhbLb^2}{m^2h^2b^2 + JL}}.$$

**Theorem 2** *Let  $U > 0$  be fixed, with  $0 < U \leq U_0$ . Then the function  $\mu(k)$  is non-increasing. Moreover, we have  $\mu(k_0) = 0$  and*

$$\lim_{k \rightarrow +\infty} \mu(k) = -\frac{U}{b}.$$

**Proof** The discriminant of (35) is

$$\Delta = \frac{mh}{J} \left[ \frac{mhb^2}{JL^2} k^2 - 2\frac{U}{L} \left( \frac{m^2h^2b^2}{JL} + 2 \right) k + \left( \frac{m^3h^3b^2U^2}{JL^2} + 4g \right) \right]. \quad (36)$$

It is not difficult to see that since  $U \leq U_0$ , then  $\Delta \geq 0$ , so that the roots of (35) are real. Hence,  $\mu(k)$  coincides with the greatest one, that is

$$\mu(k) = \lambda_2(k) = -\frac{mhb}{2JL}(mhU - k) + \frac{1}{2}\sqrt{\Delta}.$$

After some calculations, one can see that if  $U < U_0$  then

$$\lim_{k \rightarrow +\infty} \mu(k) = -\frac{U}{b}, \quad \mu(k_0) = 0 \quad \text{and} \quad \mu'(k) < 0.$$

Instead, if  $U = U_0$  one has

---

<sup>1</sup>Such a condition is  $mp \geq n$ , where  $n$  is the state space dimension,  $m$  is the input space dimension, and  $p$  is the output space dimension; in the case of (26), and with an output feedback of the form (28), we have  $p = 2$ ,  $m = 1$  and  $n = 4$ .

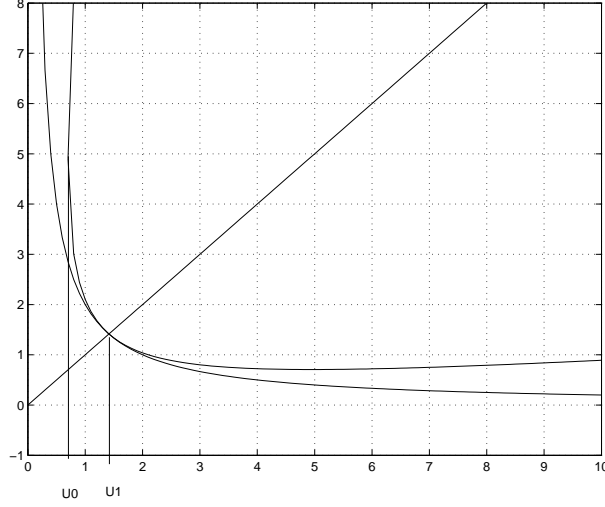


Figure 4: An example of graphical representation of the curves  $r(U)$ ,  $k = k_0(U)$  and  $\Delta(U) = 0$ . In particular, the figure shows the region of stability in the plane  $(U, k)$

$$\mu(k) = \begin{cases} \frac{U_0}{b} \left(1 - \frac{mhb^2}{lJ} k\right) & \text{for } k < \bar{k} \\ -\frac{U_0}{b} & \text{for } k \geq \bar{k} \end{cases}$$

where  $\bar{k} = \frac{m^2h^2b^2 + 2JL}{mhb^2}U_0$ . The theorem follows. Let us note just that  $\bar{k} > k_0(U_0)$ . ■

The qualitative graph of  $\mu(k)$  is shown in Figure 5 for  $0 < U < U_0$ , and in Figure 6 for  $U = U_0$ .

**Theorem 3** *Let  $U > 0$  be fixed, with  $U > U_0$ . Then  $\mu(k)$  has a minimum in the interval  $[k_0, +\infty)$ . More precisely, defining*

$$k_2 = \frac{JL^2}{mhb^2} \left[ \frac{U}{L} \left( \frac{m^2h^2b^2}{JL} + 2 \right) + \frac{2}{L} \sqrt{\left( \frac{m^2h^2b^2}{JL} + 1 \right) U^2 - \frac{mhb^2g}{J}} \right]$$

we have  $k_2 > k_0$  and

$$-\frac{U}{b} > \inf_{k > k_0} \mu(k) = \min_{k > k_0} \mu(k) = \mu(k_2) > -\frac{2U}{b} . \quad (37)$$

Moreover,

$$\mu(k_2) = -\frac{U}{b} \left[ 1 + \sqrt{1 + \frac{m^2h^2b^2}{JL} - \frac{mhgb^2}{JU^2}} \right] .$$

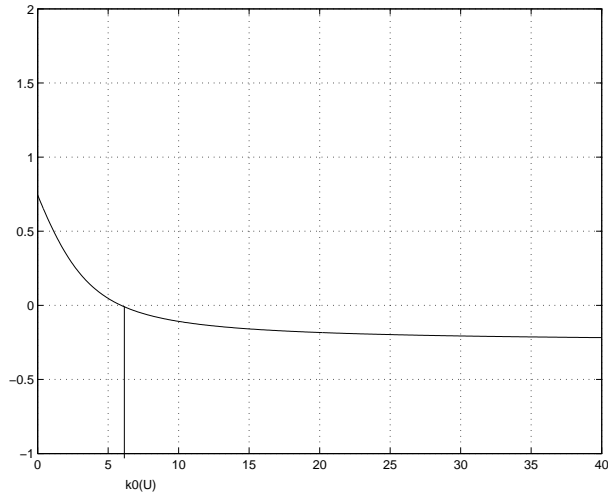


Figure 5: A typical graph of  $\mu(k)$  for  $U < U_0$

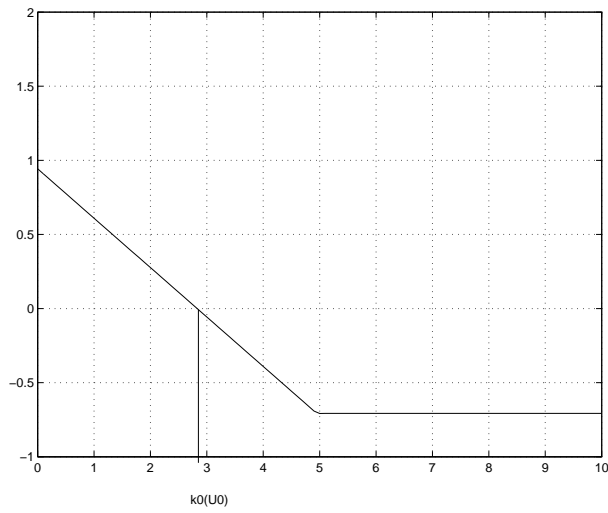


Figure 6: A typical graph of  $\mu(k)$  for  $U = U_0$

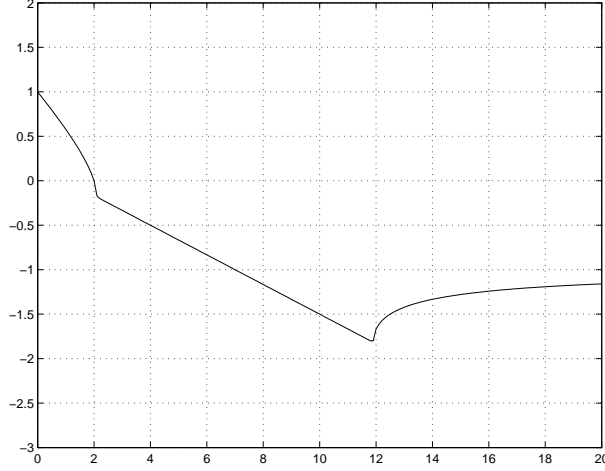


Figure 7: Typical graph of  $\mu(k)$  for  $U_0 < U < U_1$

**Proof** As in the proof of Theorem 2, we consider the discriminant  $\Delta(k)$  of (35) (see (36)). For each  $U > U_0$ , the equation  $\Delta(k) = 0$  (with respect to the unknown  $k$ ) has now two real solutions  $k_1, k_2$ , with  $k_1 < k_2$ . We have

$$k_1 < k < k_2 \implies \Delta(k) < 0 \implies \lambda_1, \lambda_2 \text{ complex conjugate}$$

$$k \leq k_1, k \geq k_2 \implies \Delta(k) \geq 0 \implies \lambda_1, \lambda_2 \text{ real.}$$

The quantities  $k_1, k_2$  are given by

$$k_1 = \frac{JL^2}{mhb^2} \left[ \frac{U}{L} \left( \frac{m^2h^2b^2}{JL} + 2 \right) - \frac{2}{L} \sqrt{\left( \frac{m^2h^2b^2}{JL} + 1 \right) U^2 - \frac{mhb^2g}{J}} \right]$$

$$k_2 = \frac{JL^2}{mhb^2} \left[ \frac{U}{L} \left( \frac{m^2h^2b^2}{JL} + 2 \right) + \frac{2}{L} \sqrt{\left( \frac{m^2h^2b^2}{JL} + 1 \right) U^2 - \frac{mhb^2g}{J}} \right].$$

In the plane  $U, k$ , the maps  $k = k_1(U)$ ,  $k = k_2(U)$  represent for  $U > U_0$  the two branches of the curve  $\Delta = \Delta(U, k) = 0$ . A direct computation shows that for each  $U > U_0$  we have  $k_1(U) \geq k_0(U)$  (so that also  $k_2(U) > k_0(U)$ ). The values  $k_1(U)$  and  $k_0(U)$  coincide only for  $U = U_1$ : more precisely, we have  $k_1(U_1) = k_0(U_1) = r(U_1)$ . We also have

$$\lim_{U \rightarrow +\infty} k_1(U) = \lim_{U \rightarrow +\infty} k_2(U) = +\infty.$$

As a further remark, we note that

$$\lim_{U \rightarrow U_0^+} k_1(U) = \lim_{U \rightarrow U_0^+} k_2(U) = \frac{m^2h^2b^2 + 2JL}{mhb^2} U_0.$$

We are now ready to discuss the shape of  $\mu(k)$ . In the interval  $[k_1, k_2]$  the decay rate  $\mu(k)$  reduces to the common real parts of the characteristic roots of (35), that is

$$\mu(k) = \frac{mhb}{2JL}(mhU - k) .$$

Hence,  $\mu(k)$  is linear and decreasing. For  $k \geq k_2$ , arguing as in the proof of Theorem 2, but taking into account that now  $U > U_0$ , one sees that  $\mu(k)$  is increasing, and

$$\lim_{k \rightarrow +\infty} \mu(k) = -\frac{U}{b} .$$

Finally, for  $k \leq k_1$ ,  $\mu(k)$  is decreasing. Thus, it is immediate to conclude that  $\mu(k)$  achieves a minimum for  $k = k_2$ .

The expression of  $\mu(k_2)$  is readily obtained for direct substitution, and it is not difficult to see that  $\mu(k_2) > -2U/b$ .

■

The qualitative graph of  $\mu(k)$  in Figure 7 for  $U_0 < U < U_1$ .

## 7 Conclusion

In this paper we studied a mathematical model of an inverted pendulum assembled on a skate. We proved that the upper equilibrium position of the pendulum can be stabilized provided that a suitable feedback law is applied in order to control the motion of the skate, and the speed of the skate is large enough. The feedback law is designed in order to mimic the centrifugal force which counteracts the displacements from the equilibrium position: hence, it is similar to the self-stability mechanism of a bicycle. However, it does not work as a steering wheel, but rather as a pair of forces applied orthogonally to the front endpoint of the skate. The discussion of the previous sections indicates that, in order to improve the stability performances, the following criteria should be adopted.

- The value of  $U_1$  should be as small as possible. One way to meet this requirement is to increase the value of  $h$  (see (33)).
- The absolute value of  $\mu(k_2)$  should be as large as possible. From (37) it is clear that this goal can be achieved by taking  $b$  as small as possible.
- The cruising speed  $U > U_0$  should be reached as soon as possible. Indeed for  $U < U_0$ , in order to improve the efficiency of the control action, a torque with larger and larger gain  $k$  should be applied.
- For  $U_0 \leq U \leq U_1$  the optimal decay rate is achieved for a finite value  $k = k_2 > 0$ .

It is worthwhile to notice that these conclusions agree with the criteria adopted in usual bicycle design and riding.

## References

- [1] *Advances in Motorcycle Design and Control*, IEEE Control Systems Magazine, **26**(5) October 2006
- [2] C.W. Anderson, *Learning to control an inverted pendulum using neural networks*, IEEE Control Systems Magazine, **9**(3) April 1989, pp. 31-37
- [3] K.J. Åström, K. Furuta, *Swinging up a pendulum by energy control*, Automatica, **36**(2) 2000, pp. 287-295
- [4] A. Bacciotti and L. Rosier, *Liapunov functions and Stability in Control Theory*, Communications in Control Engineering, Springer Verlag, London, 2005
- [5] A.M. Bloch, *Nonholonomic Mechanics and Control*, IAM, Springer, 2003
- [6] D.E.H. Jones, *The Stability of the bicycle*, Physics Today, April 1970, pp. 34-40
- [7] H.K. Khalil, *Nonlinear Systems*, Prentice Hall, 2002
- [8] M. Landry, S.A. Campbell, K. Morris, C.O. Aguilar, *Dynamics of an inverted pendulum with delayed feedback control*, SIAM J. Applied Dynamical Systems, **4**(2) 2005, pp. 333-351
- [9] J. Leventides, J. Rosenthal, X.A. Wang, *The pole placement problem via PI feedback controllers*, International Journal of Control **72**(1999), pp. 1065-1077
- [10] [http://ruina.tam.cornell.edu/research/topics/bicycle\\_mechanics](http://ruina.tam.cornell.edu/research/topics/bicycle_mechanics)
- [11] S.M. Meerkov, *Principle of vibrational control: theory and applications*, IEEE Transactions on Automatic Control, **25**(4) 1980, pp. 755-762
- [12] J.P. Meijaard, J.M. Papadopoulos, A. Ruina, A.L. Schwab, *Linearized dynamics equations for the balance and steer of a bicycle: a benchmark and review*, Proc. R. Soc. A **463**(2084) 2007, pp. 1955-1982
- [13] K. Pathak, J. Franch, S.K. Agrawal, *Velocity and position control of a wheeled inverted pendulum by partial feedback linearization*, IEEE Transaction on Robotics, **21**(3) 2005, pp. 505-513
- [14] B. Shapiro, B.T. Zinn, *High-frequency nonlinear vibrational control*, IEEE Transactions on Automatic Control, **42**(1) 1997, pp. 83-90
- [15] Sontag E.D., *Mathematical Control Theory*, Springer Verlag, New York, 1990